

# Influence of heat- and mass-transfer coupling on the optimal performance of a non-isothermal chemical engine

Yanhua Cai, Guozhen Su,\* and Jincan Chen

*Department of Physics and Institute of Theoretical Physics and Astrophysics,  
Xiamen University, Xiamen 361005, People's Republic of China,*

*\*e-mail: gzs@xmu.edu.cn*

Recibido el 5 de noviembre de 2009; aceptado el 16 de junio de 2010

The cyclic model of a non-isothermal chemical engine operated between two reservoirs with different temperatures and chemical potentials is established, in which the irreversibilities resulting from the heat and mass transfer between the working fluid and the reservoirs are taken into account. Expressions for the power output and efficiency of the engine are analytically derived and used to analyze the performance characteristics of the engine at the maximum power output. The general characteristics of the efficiency of the engine are searched in detail. The optimal criteria for some important parameters, such as the power output and efficiency, are obtained and the reasonably operating region of the engine is determined. Some interesting cases are specially discussed. The results obtained here can reveal the performance characteristics of a non-isothermal chemical engine affected by the irreversibilities of heat- and mass-transfer coupling.

*Keywords:* Chemical engine; heat- and mass-transfer coupling; irreversibility; maximum power output; optimum characteristic.

Se establece el modelo cíclico de un motor químico no isotérmico operado entre dos reservorios a diferente temperatura y potencial químico, donde se toman en cuenta las irreversibilidades que son resultado de la transferencia de masa y calor entre el fluido de trabajo y los reservorios. Se obtienen analíticamente expresiones para la generación de poder y la eficiencia del motor y se utilizan para analizar las características de desempeño del motor cuando la generación de poder es máxima. Se hace una búsqueda detallada de las características de eficiencia del motor. Se obtienen criterios óptimos para algunos parámetros, tales como la generación de poder y la eficiencia, y se determina la región de operación razonable para el motor. Se discuten algunos casos de interés. Los resultados obtenidos revelan características de desempeño de un motor térmico no isotérmico afectado por irreversibilidades del acoplamiento de transferencia de masa y calor.

*Descriptores:* Motor químico; acoplamiento de transferencia de calor y masa; irreversibilidad; potencia máxima de salida; óptimo característico.

PACS: 05.70.Ln; 07.20.Pe; 05.07.-a

## 1. Introduction

One of the classical problems of thermodynamics is to investigate the efficiency of heat engines at the maximum work output. The theory of heat engines is one of the main roots of modern thermodynamics [1]. Recently, the study of the maximum power characteristics of various thermodynamic systems [2-11] including heat engines, chemical engines, thermal Brownian motors, and so on, has been a considerable renewed interest. Many authors have investigated the influence of heat-transfer irreversibility and other irreversible losses on the maximum power output and other optimal performance of heat engines [12-21] and obtained the optimally operating criteria of heat engines [22-25]. In addition, the study of heat engines has been successfully extended to the case of isothermal chemical engines [26-32] and some significant results have been obtained.

On the basis of the irreversible cycle models of heat engines and isothermal chemical engines, some authors have respectively established several different cycle models [8,33-36] of non-isothermal chemical engines with heat- and mass- transfer coupling. Owing to the complexity of heat- and mass-transfer coupling, many performance characteristics of non-isothermal chemical engines have not been understood well, and consequently, a great deal of research

related to non-isothermal chemical engines needs to be further carried out.

In the present paper, we will extend the previous works to establish a simplified cycle model of an irreversible non-isothermal chemical engine, which can be used to reveal the influence of heat- and mass-transfer coupling on the performance of the cycle system. The new results obtained are different from those derived from the existing models of not only the pure heat or chemical engines but also the heat- and mass-transfer combined engines [8,33-36]. The concrete contents of the paper are organized as follows: In Sec. 2, we outline the cyclic model of an irreversible non-isothermal chemical engine, where the coupling irreversibilities in the heat- and mass-transfer processes are taken into account. In Sec. 3, general expressions for the power output and efficiency of the cycle system are analytically derived. In Secs. 4 and 5, the maximum power output is calculated and the general characteristics of the efficiency varying with the working parameters and chemical potentials are analyzed in detail, respectively. In Sec. 6, the power output versus efficiency characteristics are revealed, from which the reasonably operating region of the cycle system is determined. In Sec. 7, two special cases of the cycle system are discussed, and consequently, some important conclusions in literature are directly derived. In Sec. 8, some summarized conclusions are given.

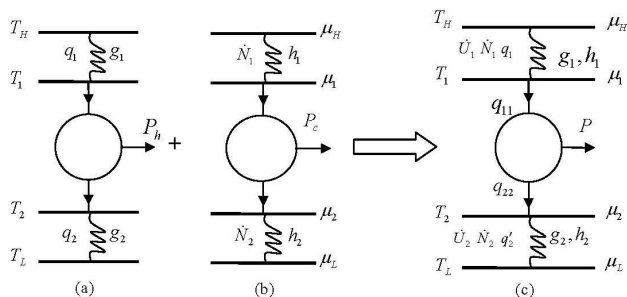


FIGURE 1. Schematic diagrams of an irreversible chemical engine with finite-rate heat and/or mass transfer.

## 2. The cyclic model of an irreversible chemical engine

Figure 1 shows the schematic diagrams of heat and/or chemical engines operated between two different reservoirs. In Fig. 1a, the heat engine is operated between two heat reservoirs at temperatures  $T_H$  and  $T_L$  ( $T_H > T_L$ ), where  $q_1$  and  $q_2$  are, respectively, the rates of the heat input and output of the cycle,  $T_1$  and  $T_2$  are, respectively, the temperatures of the working fluid in the high- and low-temperature isothermal processes of the cycle,  $g_1$  and  $g_2$  are, respectively, the thermal coefficients between the heat engine and the two heat reservoirs, and  $P_h$  is the power output of the cycle. This idealized cycle model has been widely adopted to investigate the optimal performance of irreversible heat engines [19,22-24,37] and some important results have been obtained. In Fig. 1b, the chemical engine is operated between two mass reservoirs with chemical potentials  $\mu_H$  and  $\mu_L$  ( $\mu_H > \mu_L$ ), where  $\dot{N}_1$  and  $\dot{N}_2$  are the rates of the mass input and output of the cycle,  $\mu_1$  and  $\mu_2$  are, respectively, the chemical potentials of the working fluid in the two constant chemical potential processes of the cycle,  $h_1$  and  $h_2$  are, respectively, the mass-transfer coefficients between the chemical engine and the two mass reservoirs, and  $P_c$  is the power output of the cycle. This simplified cycle model was first proposed by De Vos [33] and adopted and generalized by other researchers [26-30] to discuss the optimal performance of an isothermal chemical engine and some significant results have been obtained. The cycle shown in Fig. 1c is the coupling system [33] of the heat engine shown in Fig. 1a and the chemical engine shown in Fig. 1b. It is a non-isothermal chemical engine, which is operated between two reservoirs at different temperatures and chemical potentials. In Fig. 1c,  $\dot{U}_1$  and  $\dot{U}_2$  are the rates of the energy input and output of the cycle,  $q_{11}$  and  $q_{22}$  are the rates of the heat input and output of the cycle,  $q'_2$  is the rate of the heat flow rejected to the low-temperature heat reservoir,  $P$  is the power output of the cycle, and other signs are the same as those adopted in Figs. 1a and 1b. It is worthwhile to note that  $q_{11}$  and  $q_{22}$  are, respectively, different from  $q_1$  and  $q'_2$  because there exists mass transfer in the cycle.

For a non-isothermal chemical engine shown in Fig. 1c, one can obtain the following relations:

$$T_H \geq T_1 \geq T_2 \geq T_L \tag{1}$$

and

$$\mu_H \geq \mu_1 \geq \mu_2 \geq \mu_L. \tag{2}$$

Obviously, Fig. 1c is a more general model. When  $\mu_H = \mu_L$ , Fig. 1c is reduced to Fig. 1a. When  $T_H = T_L$ , Fig. 1c is reduced to Fig. 1b. Thus, when the cycle model shown in Fig. 1c is used to discuss the optimal performance of an irreversible non-isothermal chemical engine, we can obtain some important results which are of general significance.

## 3. Expressions of the power output and efficiency

In order to discuss the influence of finite-rate heat and mass transfers on the performance of the cycle, it is often assumed that both heat and mass transfers satisfy linear laws [21-25,26-28,30], and consequently, the heat- and mass-transfer equations in the cycle may be expressed as

$$q_1 = g_1 (T_H - T_1), \tag{3}$$

$$q_2 = g_2 (T_2 - T_L), \tag{4}$$

$$\dot{N}_1 = h_1 (\mu_H - \mu_1), \tag{5}$$

and

$$\dot{N}_2 = h_2 (\mu_2 - \mu_L). \tag{6}$$

According to the energy and mass conservations, we can obtain

$$\dot{U}_1 = \dot{U}_2 + P, \tag{7}$$

$$\dot{N}_1 = \dot{N}_2 \equiv \dot{N}, \tag{8}$$

$$\dot{U}_1 = q_1 + \mu_H \dot{N} = q_{11} + \mu_1 \dot{N}, \tag{9}$$

and

$$\dot{U}_2 = q_{22} + \mu_2 \dot{N} = q'_2 + \mu_L \dot{N}. \tag{10}$$

According to the second law of thermodynamics, one can obtain

$$\frac{q_1}{T_1} = \frac{q_2}{T_2} \tag{11}$$

and

$$\frac{q_{11}}{T_1} = \frac{q_{22}}{T_2}. \tag{12}$$

Using the above equations, we can derive the three heat flows  $q_{11}$ ,  $q_{22}$  and  $q'_2$  and the power output  $P$  and efficiency

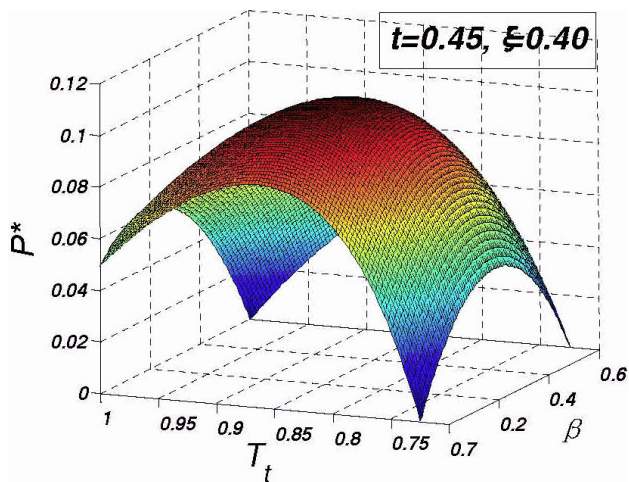


FIGURE 2. The three-dimensional diagram of the dimensionless power output  $P^* = P / (h_1 \mu_H^2)$  varying with variables  $T_t$  and  $\beta$ , where the parameters  $a = 1, b = 1, k = 1, t = 0.45$  and  $\xi = 0.4$ .

$\eta$  of the non-isothermal chemical engine

$$q_{11} = g_1(T_H - T_1) + (\mu_H - \mu_1) \dot{N}, \tag{13}$$

$$q_{22} = g_2(T_2 - T_L) + (\mu_H - \mu_1) \dot{N} \frac{T_2}{T_1}, \tag{14}$$

$$q'_2 = g_2(T_2 - T_L) + \left[ (\mu_2 - \mu_L) + (\mu_H - \mu_1) \frac{T_2}{T_1} \right] \dot{N}, \tag{15}$$

$$P = h_1 \mu_H^2 \left\{ \frac{[a + t - (1+a)T_t][k(1 - T_t) + X^2]}{a - (1+a)T_t} + \beta X \right\}, \tag{16}$$

and

$$\eta = \frac{P}{\dot{U}_1} = \frac{[a + t - (1+a)T_t][k(1 - T_t) + X^2]}{[a - (1+a)T_t][k(1 - T_t) + X]} + \frac{\beta X}{k(1 - T_t) + X}, \tag{17}$$

respectively, where

$$a = g_1/g_2, \quad b = h_1/h_2, \quad t = T_L/T_H, \quad \xi = \mu_L/\mu_H,$$

$$k = g_1 T_H / (h_1 \mu_H^2), \quad T_t = T_1/T_H,$$

$$\beta = (\mu_1 - \mu_2) / \mu_H, \quad X = (1 - \xi - \beta) / (b + 1),$$

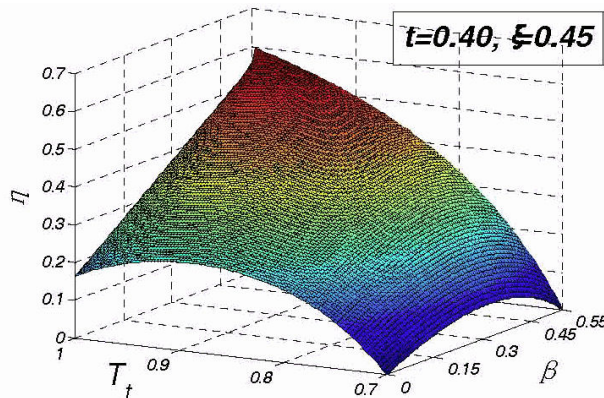
$$\text{and } (a + t) / (1 + a) \leq T_t \leq 1.$$

### 4. Maximum power output

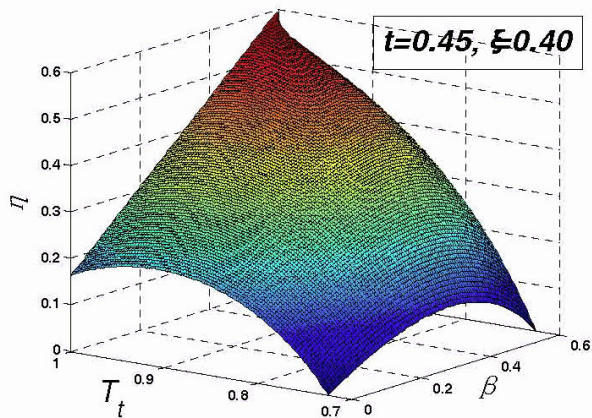
It is seen from Eq. (16) that the power output is a function of two variables ( $T_t, \beta$ ) for other given parameters  $a, b, t, \xi$  and  $k$ . Using Eq. (16), we can plot the three-dimensional diagram of the dimensionless power output  $P^* = P / (h_1 \mu_H^2)$  varying with the parameters  $T_t$  and  $\beta$ , as shown in Fig. 2. It is clearly seen from Fig. 2 that there exist the optimum values  $T_{t,m}$  and  $\beta_m$  of  $T_t$  and  $\beta$  at which the power output attains its maximum. From Eq. (16) and the extremal conditions  $(\partial P / \partial \beta)_{T_t} = 0$  and  $(\partial P / \partial T_t)_{\beta} = 0$ , one can find that these

optimum values of  $\beta$  and  $T_t$  at the maximum power output are, respectively, determined by

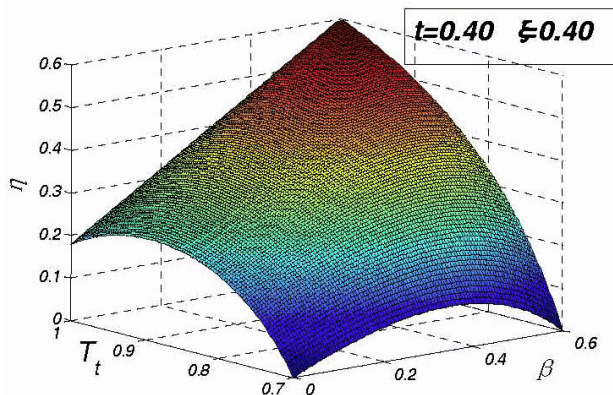
$$\beta_m = \left( \frac{1 - \xi}{2} \right) \left( 1 - \frac{1 + C}{b - C} \right) \tag{18}$$



(a)



(b)



(c)

FIGURE 3. The three-dimensional diagrams of the efficiency  $\eta$  varying with variables  $T_t$  and  $\beta$  for (a)  $t = 0.4$  and  $\xi = 0.45$ , (b)  $t = 0.45$  and  $\xi = 0.4$  and (c)  $t = 0.4$  and  $\xi = 0.4$ , where the parameters  $a = 1, b = 1$  and  $k = 1$ .

and

$$A_4 T_{t,m}^4 + A_3 T_{t,m}^3 + A_2 T_{t,m}^2 + A_1 T_{t,m} + A_0 = 0, \quad (19)$$

where

$$\begin{aligned} C &= t[a - (1 + a)T_{t,m}]^{-1}, \\ A_0 &= 4k(a^2 - t)(ab - t)^2 - ta^2(1 + a)(1 - \xi)^2, \\ A_1 &= 8k(1 + a)(ab - t)[b(t - a^2) - a(ab - t)] \\ &\quad + 2at(1 + a)^2(1 - \xi)^2, \\ A_2 &= 4k(1 + a)^2[6ab(ab - t) + t(t - b^2)] \\ &\quad - t(1 + a)^3(1 - \xi)^2, \\ A_3 &= 8kb(1 + a)^3(t - 2ab), \quad \text{and} \\ A_4 &= 4kb^2(1 + a)^4. \end{aligned}$$

Substituting Eqs. (18) and (19) into Eqs.(16) and (17), we can obtain the maximal power output and the corresponding efficiency

$$P_{\max} = h_1 \mu_H^2 \left[ k(1 - T_{t,m})(1 + C) + \frac{(1 - \xi)^2}{4(b - C)} \right] \quad (20)$$

and

$$\eta_m = \frac{4k(1 - T_{t,m})(b - C)(1 + C) + (1 - \xi)^2}{4k(1 - T_{t,m})(b - C) + 2(1 - \xi)}, \quad (21)$$

respectively.

### 5. General characteristics of the efficiency

Using Eq. (17), we can plot the three-dimensional diagrams of the efficiency  $\eta$  varying with the parameters  $T_t$  and  $\beta$ , as shown in Fig. 3. It is seen from Fig. 3 that the efficiency  $\eta$  is a monotonically increasing function of  $\beta$  when  $T_t = 1$  and the efficiency  $\eta$  is also a monotonically increasing function of  $T_t$  when  $\beta = 1 - \xi$ . When  $T_t = 1$  and  $\beta = 1 - \xi$ , the efficiency  $\eta$  attains its maximum, *i.e.*,

$$\eta = \eta_{\max} = \eta_r = \begin{cases} 1 - T_L/T_H \equiv \eta_{r1}, & (t > \xi) \\ 1 - \mu_L/\mu_H \equiv \eta_{r2}, & (t < \xi) \end{cases}, \quad (22)$$

where  $\eta_r$  is the reversible efficiency of the cycle and  $\eta_{r1}$  and  $\eta_{r2}$  are the reversible efficiencies of the Carnot heat engine and the isothermal chemical engine, respectively. When  $T_t < 1$  and  $\beta < 1 - \xi$ , the relation between the efficiency and the parameters  $T_t$  and  $\beta$  is complex. Thus, it is necessary to discuss further the characteristics of the efficiency for the three cases of  $t < \xi$ ,  $t > \xi$ , and  $t = \xi$ , respectively.

#### 5.1. The case of $t < \xi$

For the case of  $t < \xi$ , the general characteristics of the efficiency can be directly seen from Fig. 3a. When  $T_{t,c} \leq T_t < 1$ ,

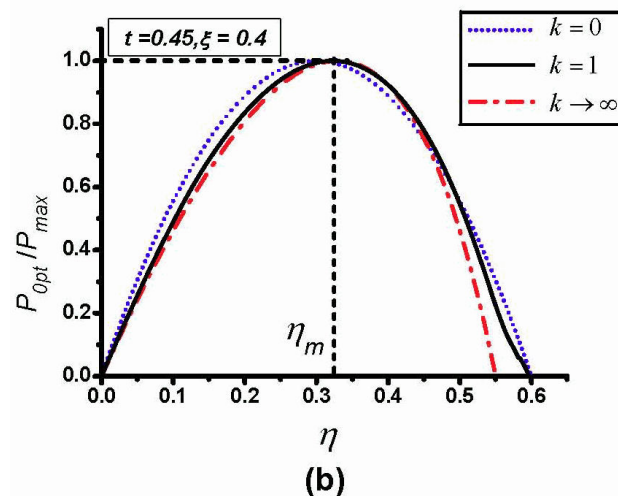
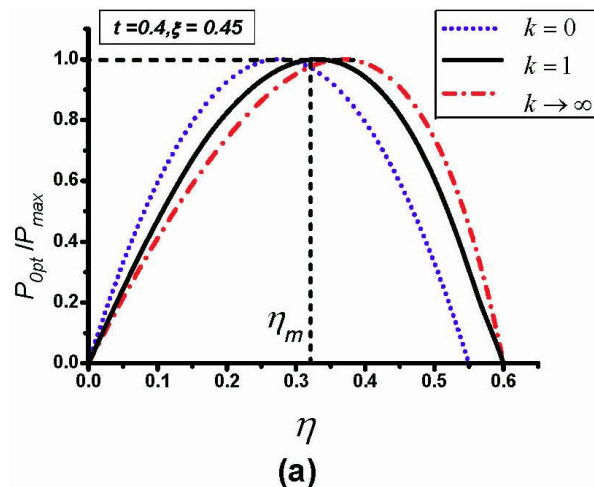


FIGURE 4. The dimensionless optimized power output  $P_{opt}/P_{max}$  versus efficiency  $\eta$  for (a)  $t = 0.4$  and  $\xi = 0.45$  and (b)  $t = 0.45$  and  $\xi = 0.4$ , where the parameters  $a = 1$  and  $b = 1$ .

$\eta$  is a monotonically increasing function of  $\beta$ , where  $T_{t,c}$  is a critical parameter determined by

$$\begin{aligned} T_{t,c} &= 1 - \frac{1}{2b} \\ &\times \left[ \frac{b+t}{1+a} + \frac{\xi}{k} - \sqrt{\left( \frac{b+t}{1+a} + \frac{\xi}{k} \right)^2 + \frac{4b(t-\xi)}{k(1+a)}} \right]. \quad (23) \end{aligned}$$

For the parameters adopted in Fig. 3a,  $T_{t,c} \approx 0.98$ . When  $(a + t)/(a + 1) \leq T_t < T_{t,c}$ , there exists an optimal value  $\beta_{opt,\eta}$  of  $\beta$  at which the efficiency attains its local maximum, where  $\beta_{opt,\eta}$  is given by

$$\begin{aligned} \beta_{opt,\eta} &= 1 - \xi - (b + 1) \\ &\times \left[ \sqrt{1 + k(1 - T_t) + (b + \xi)\{t[a - (1 + a)T_t]^{-1} - b\}^{-1}} \right. \\ &\quad \left. - k(1 - T_t) \right]. \quad (24) \end{aligned}$$

When  $\beta < 1 - \xi$ , there always exists the local maximum of the efficiency and the corresponding optimum value  $T_{t,opt,\eta}$

of  $T_t$ , where  $T_{t,opt,\eta}$  is given by

$$T_{t,opt,\eta} = 1 + \frac{BX - \sqrt{ktX(B-A)[k(1+a)^{-1} + X^2]}}{kA} \quad (25)$$

with

$$A = kt - (1+a)X(bX + \xi), \quad \text{and} \quad B = k[(b+t)X + \xi].$$

$$\beta_c = 1 - \xi - \frac{(1+b)\{\sqrt{4kb(1+a)(t-\xi) + [k(b+t) + (1+a)\xi]^2} - [k(b+t) + (1+a)\xi]\}}{2b(1+a)}. \quad (26)$$

For the parameters adopted in Fig. 3b,  $\beta_c \approx 0.56$ . When  $0 \leq \beta < \beta_c$ , there exists an optimum value  $T_{t,opt,\eta}$  of  $T_t$  at which the efficiency attains its local maximum, where  $T_{t,opt,\eta}$  is given by Eq. (25). When  $T_t < 1$ , there exists an optimum value  $\beta_{opt,\eta}$  of  $\beta$  at which the efficiency  $\eta$  attains its local maximum, where  $\beta_{opt,\eta}$  is given by Eq. (24).

**5.3. The case of  $t = \xi$**

In this case, there exist the optimum values  $T_{t,opt,\eta}$  and  $\beta_{opt,\eta}$  of  $T_t$  and  $\beta$  at which  $\eta$  attains its local maximum, where  $T_{t,opt,\eta}$  and  $\beta_{opt,\eta}$  are, respectively, given by Eqs. (24) and (25).

**6. Optimally operating regions**

Using Eqs. (16) and (17), we can obtain the relationship between the power output and the efficiency as

$$P = f[T_t, \beta(\eta, T_t)] \quad (27)$$

and generate the characteristic curves of the dimensionless optimized power output  $P_{opt}/P_{max}$  varying with the efficiency  $\eta$  through numerical computation, as shown in Fig. 4, where  $P_{max}$  is the maximum power output of the system and  $P_{opt}$  is the optimized power output, *i.e.*, the local maximum of the power output for a given efficiency. It is seen from Figs. 4a and 4b that there always exist a maximum power output  $P_{max}$  and a corresponding efficiency  $\eta_m$ . When the power output of the cycle is smaller than the maximum power output  $P_{max}$ , there are two different efficiencies for a given power output, where one is larger than  $\eta_m$  and the other is

**5.2. The case of  $t > \xi$**

For the case of  $t > \xi$ , Fig. 3b can be used to analyze the general characteristics of the efficiency. When  $\beta_c \leq \beta < 1 - \xi$ , the efficiency  $\eta$  is a monotonically increasing function of  $T_t$ , where the critical parameter  $\beta_c$  is given by

smaller than  $\eta_m$ . When the efficiency of the cycle attains the reversible efficiency  $\eta_r$ , the power output is equal to zero. For a real system, although the efficiency of the cycle cannot attain the reversible efficiency  $\eta_r$ , it should be required to be not smaller than  $\eta_m$ . When the efficiency of the cycle is smaller than  $\eta_m$ , the power output will decrease as the efficiency of the cycle is decreased. It is thus clear that the optimal region of the efficiency should be situated between  $\eta_m$  and  $\eta_r$ , *i.e.* [22,23],

$$\eta_m \leq \eta < \eta_r. \quad (28)$$

When the cycle is operated in such a region, the power output will increase as the efficiency of the cycle is decreased, and vice versa. It indicates that  $\eta_m$  is an important parameter of a non-isothermal chemical engine and determines the lower bound of the optimized efficiency.

According to Eq. (28) one can further determine the optimal regions of other parameters as follows:

$$T_{1m} \leq T_1 < T_H, \quad (29)$$

$$T_L < T_2 < T_{2m}, \quad (30)$$

and

$$\beta_m \leq \beta < 1 - \xi, \quad (31)$$

where  $T_{1m}, T_{2m}$  and  $\beta_m$  are the values of the parameters  $T_1, T_2$  and  $\beta$  at the maximum power output  $P_{max}$ , respectively. For some given values of other parameters, the values of  $P_{max}/(h_1\mu_H^2)$ ,  $\eta_m, T_{1m}/T_H, T_{2m}/T_L$  and  $\beta_m$  are easily obtained by the numerical calculation, as listed in Table I.

TABLE I. The values of  $P_{max}/(h_1\mu_H^2), \eta_m, T_{1m}/T_H, T_{2m}/T_L$  and  $\beta_m$  for the case of  $a = 1$  and  $b = 1$ .

	$k$	$P_{max}/(h_1\mu_H^2)$	$\eta_m$	$T_{1m}/T_H$	$T_{2m}/T_L$	$\beta_m$
t=0.4 $\xi=0.45$	0.5	0.08060	0.3166	0.8345	1.247	0.2063
	1	0.1141	0.3317	0.8256	1.268	0.2107
	2	0.1815	0.3437	0.8207	1.280	0.2110
t=0.45 $\xi=0.4$	0.5	0.08164	0.3196	0.8574	1.200	0.2317
	1	0.1084	0.3226	0.8462	1.222	0.2357
	2	0.1624	0.3256	0.8409	1.233	0.2389

### 7. Two special cases

The results obtained above are general, from which some conclusions in literature can be easily derived.

- (1) When  $T_H = T_L, T_t = 1$  and the cycle system reduces to an isothermal chemical engine. Eqs. (16) and (17) can be, respectively, simplified as

$$P = h_1 \mu_H^2 \beta (1 - \xi - \beta) / (b + 1) \tag{32}$$

and

$$\eta = \beta, \tag{33}$$

which are just the expressions of the power output and efficiency of a chemical engine [30]. It is interesting to note that the optimal relations of an isothermal chemical engine are the same as those of a non-isothermal chemical engine under the condition of  $g_1 = 0$ . The optimized power output versus efficiency curves are shown by the curves of  $k = 0$  in Fig. 4. The maximum power output [28,30]

$$P_{\max} = \frac{h_1 \mu_H^2 (1 - \xi)^2}{4(b + 1)} \tag{34}$$

and the corresponding efficiency

$$\eta_m = \frac{1}{2}(1 - \xi) = \frac{1}{2}\left(1 - \frac{\mu_L}{\mu_H}\right). \tag{35}$$

can be directly derived from Eqs. (32) and (33).

- (2) When  $\mu_H = \mu_L, \beta = 0$  and the cycle system reduces to a pure heat engine. Eqs. (16) and (17) can be, respectively, simplified as

$$P = \frac{g_1 T_H (1 - T_t) [a + t - (1 + a) T_t]}{a - (1 + a) T_t} \tag{36}$$

and

$$\eta = \frac{a + t - (1 + a) T_t}{a - (1 + a) T_t}, \tag{37}$$

which are just the expressions of the power output and efficiency of a heat engine [23]. It is also interesting

to note that the optimal relations of a pure heat engine are the same as those of a non-isothermal chemical engine under the condition of  $h_1 = 0$ . The optimized power output versus efficiency curves are shown by the curves of  $k \rightarrow \infty$  in Fig. 4. The maximum power output [22-25,37,38]

$$P_{\max} = \frac{g_1 T_H (1 - \sqrt{t})^2}{1 + a} \tag{38}$$

and the corresponding efficiency

$$\eta_m = 1 - \sqrt{t} \equiv \eta_{CA} \tag{39}$$

can be directly derived from Eqs. (36) and (37).

### 8. Conclusions

With the help of the current cycle models of heat engines affected by finite-rate heat transfer and isothermal chemical engines affected by finite-rate mass transfer, the generalized cyclic model of an irreversible non-isothermal chemical engine with heat- and mass-transfer coupling has been established, from which the power output and efficiency of the system have been analytically derived. The influence of the irreversibilities in the heat- and mass-transfer processes on the performance of the cycle system is discussed. The power output and efficiency are optimized with respect to the temperatures and chemical potentials of the working substance and some important parameters, such as the maximum power output and the corresponding efficiency, are analytically calculated. The characteristic curves of the power output versus efficiency are presented, from which the optimally operating region of the non-isothermal chemical engine is determined. The results obtained are novel and general. They can reveal the fundamental characteristics of a non-isothermal chemical engine and provide some new theoretical guidance for the optimal design and operation of realistic systems.

### Acknowledgments

This work has been supported by the National Natural Science Foundation (No. 10875100), People's Republic of China.

---

1. R.Filliger and P. Reimann, *Phys. Rev. Lett.* **99** (2007) 230602.  
 2. C. Van den Broeck, *Phys. Rev. Lett.* **95** (2005) 190602.  
 3. G. Aragon-Gonzalez, A. Canales-Palma, A. Leon-Galicia, and J.R. Morales-Gomez, *Rev. Mex. Fis.* **52** (2006) 309.  
 4. B. Jimenez de Cisneros and A.C. Hernandez, *Phys. Rev. Lett.* **98** (2007) 130602.  
 5. B. Jimenez de Cisneros and A.C. Hernandez, *Phys. Rev. E* **77** (2008) 041127.  
 6. M.A. Barranco-Jimenez, N. Sanchez-Salas, and F. Angulo-Brown, *Rev. Mex. Fis.* **54** (2008) 284.  
 7. T. Schmiedl and U. Seifert, *Eur. Phys. Lett.* **81** (2008) 20003.  
 8. M. Esposito, K. Lindenberg, and C. Van den Broeck, *Phys. Rev. Lett.* **102** (2009) 130602.  
 9. L. Chen, H. Song, F. Sun, and S. Wang, *Rev. Mex. Fis.* **55** (2009) 55.

10. A. Gomez-Marin and J.M. Sancho, *Phys. Rev. E* **74** (2006) 062102.
11. I. Derényi, M. Bier, and R. Dean Astumian, *Phys. Rev. Lett.* **83** (1999) 903.
12. M. Huleihil and B. Andresen, *J. Appl. Phys.* **100** (2006) 014911.
13. M. Asfaw and M. Bekele, *Phys. Rev. E* **72** (2005) 056109.
14. Y. Zhang, B. Lin, and J. Chen, *J. Appl. Phys.* **97** (2005) 084905.
15. L.A. Arias-Hernandez and F. Angulo-Brown, *J. Appl. Phys.* **81** (1997) 2973.
16. A. Bejan, *J. Appl. Phys.* **79** (1996) 1191.
17. M.A. Ait-Ali, *J. Appl. Phys.* **78** (1995) 4313.
18. F. Romm, *J. Appl. Phys.* **74** (1993) 5310.
19. J. Chen, *J. Phys. A* **31** (1998) 3383.
20. Z. Yan and J. Chen, *J. Chem. Phys.* **92** (1990) 1994.
21. J. Chen and Z. Yan, *Phys. Rev. A*, **39** (1988) 4140.
22. J. Chen, Z. Yan, G. Lin, and B. Andresen, *Energy Convers. Manage.* **42** (2001) 173.
23. A. de Vos, *Endoreversible thermodynamics of solar energy conversion* (Oxford: Oxford University Press, 1992).
24. M.H. Rubin, *Phys. Rev. A* **19** (1979) 1272.
25. F.L. Curzon and B. Ahlborn, *Am. J. Phys.* **43** (1975) 22.
26. J.M. Gordon, *J. Appl. Phys.* **73** (1993) 8.
27. J.M. Gordon and V.N. Orlov, *J. Appl. Phys.* **74** (1993) 5303.
28. L. Chen, F. Sun, and C. Wu, *J. Phys. D: App. Phys.* **31** (1998) 1595.
29. E.J. Delgado, *J. Appl. Phys.* **85** (1999) 7467.
30. G. Lin, J. Chen, and E. Bruck, *Appl. Energy* **78** (2004) 123.
31. G. Lin, J. Chen, and B. Hua, *Appl. Energy* **72** (2002) 359.
32. S. Xia, L. Chen, and F. Sun, *J. Appl. Phys.* **105** (2009) 124905.
33. A. De Vos, *J. Phys. Chem.* **95** (1991) 4534.
34. T.E. Humphrey, R. Newbury, R.P. Taylor, and H. Linke, *Phys. Rev. Lett.* **89** (2002) 116801.
35. S. Sieniutycz, *Int. J. Heat Mass Transfer* **51** (2008) 5859.
36. S. Sieniutycz, *Int. J. Heat Mass Transfer* **52** (2009) 2453.
37. A. De Vos, *J. Phys. D: App. Phys.* **20** (1987) 232.
38. L. Chen and Z. Yan, *J. Chem. Phys.* **90** (1989) 3740.